

# MODELING A BACTERIUM'S LIFE: A PETRI-NET LIBRARY IN MODELICA

Sabrina Proß<sup>1)</sup>, Bernhard Bachmann<sup>1)</sup>, Ralf Hofestädt<sup>2)</sup>, Karsten Niehaus<sup>2)</sup>, Rainer Ueckerdt<sup>1)</sup>,  
Frank-Jörg Vorhölter<sup>2)</sup>, Petra Lutter<sup>2)</sup>

<sup>1)</sup> University of Applied Sciences  
Am Stadtholz 24  
33609 Bielefeld, Germany

sabrina.pross@fh-bielefeld.de

<sup>2)</sup> Bielefeld University  
POB 100 131  
33501 Bielefeld, Germany

plutter@cebitec.uni-bielefeld.de

## Abstract

For modeling biological systems the already existing Petri Net Libraries were further developed with OpenModelica using the SimForge graphical user interface (GUI). The Petri Nets elements were wrapped into models for different reaction types to simplify the modeling process. Additionally, a database connection was implemented for integrating kinetic data. The application of this new Reaction Library is demonstrated by the xanthan production of the bacterium *Xanthomonas campestris* pv. *campestris*. A mathematical model is introduced to predict growth and xanthan production, given an initial glucose concentration. The parameters of this model are estimated with the aid of the Optimization Toolbox in MATLAB.

## 1. Introduction

### 1.1. Biological Background

The organism under study, *Xanthomonas*, is a gram negative bacterium of the *Xanthomonadaceae*-family. It is yellow pigmented, rod shaped and has one polar flagellum (see Figure 1).

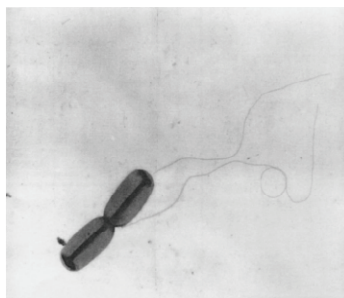


Figure 1: Electron micrograph of *Xanthomonas campestris* [1]

It grows under aerobic conditions and its genome contains about 5 million base pairs [2]. *Xanthomonas* belongs to a group of bacteria that have adopted a plant pathogenic lifestyle. Specifically, *Xanthomonas campestris* pathovar *campestris* harms cruciferous plants like cabbage and cauliflower. Besides its importance as a phytopathogen, *Xanthomonas campestris* pv. *campestris* is known as the producer of the exopolysaccharide xanthan. Xanthan (E-415) is industrially produced and of high commercial significance. e.g. it is employed as a thickening agent and emulsifier. Although substantial efforts have been put into understanding the xanthan synthesis [1], the bacterium's life strategies are far from being well understood.

### 1.2. Theoretical Background

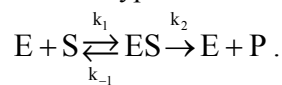
To describe the influence of external parameters on the production of substances needed for the xanthan synthesis, different kinetic models have been proposed. Unstructured kinetic models consider the bacterium's consumption of food (carbon and nitrogen sources), its growth and its xanthan production through a set of differential equations. As this minimal set of equations treats the bacterium's metabolism as a black box, more complex models had to be established. Garcia-Ochoa et al. introduced a structured kinetic model for *X. campestris* growth that is able to predict different growth rates according to different initial nitrogen concentrations [3]. As we are interested in the question under which circumstances the bacterium's focus is growth on the one hand and which factors lead to xanthan production on the other hand, we still include more details. With a complete genome sequence at hand, the biosynthesis pathways for the production of the exopolysaccharide xanthan could be elucidated

[2]. Consequently, we are enabled to set up all the metabolic pathways in question.

## 2. Methods

### 2.1. Michaelis-Menten-Kinetics

Once the metabolic pathways are clear, appropriate kinetic equations have to be assigned. As Michaelis-Menten-Kinetics has worked well with similar organisms, we have concentrated on this equation type. The basic reaction describes the transformation of a substrate into a product under enzymatic influence. At this juncture, the following reaction type is the basis:



A substrate S links to the active center of the enzyme E and forms an enzyme-substrate-complex ES. ES is converted to the product P,  $k_i$  denote velocity constants. The enzyme is set free and can link to another substrate again.

The Michaelis-Menten-Kinetic has the following form:

$$v = -\frac{d[S]}{dt} = \frac{d[P]}{dt} = \frac{k_{cat} \cdot [E] \cdot [S]}{K_m + [S]}, \quad \text{where}$$

$[S]$ ,  $[P]$  and  $[E]$  are the concentrations of substrate, product and enzyme, respectively. The parameter  $k_{cat}$  is denoted as turnover number and specifies the number of substrate molecules that one enzyme molecule converts per second if it is completely saturated with substrate. The Michaelis-Menten constant  $K_m$  is the substrate concentration at half-maximum reaction rate (see Figure 2).

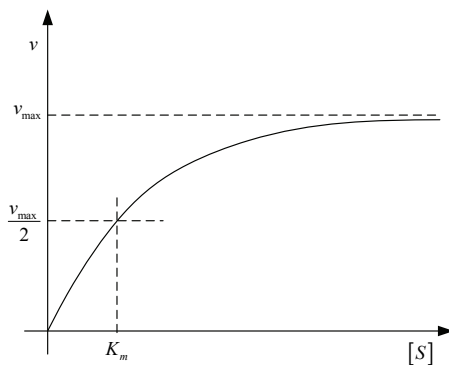


Figure 2: Michaelis-Menten diagram

The negative substrate change is equivalent to the positive product change. It is assumed that

the concentrations of free enzymes and enzyme-substrate-complexes do not change during time. They are in a steady state.

### 2.2. Growth kinetics

For modeling the growth of *Xanthomonas* bacteria it is taken into account that there is a relationship between the exhaustion of glucose and the end of growth. Therefore, two different nutrient limited Growth Kinetics are examined. The first is known as Monod Kinetics [4]:

$$\frac{d[B]}{dt} = [B] \frac{\mu \cdot [N_l]}{K_{N_l} + [N_l]}, \quad \text{where } [B] \text{ is the}$$

microbial concentration (biomass),  $[N_l]$  is the concentration of the limiting nutrient,  $\mu$  is the maximum specific growth rate and  $K_{N_l}$  is the nutrient concentration at half-maximum specific growth rate.

The second has the following form [5]:

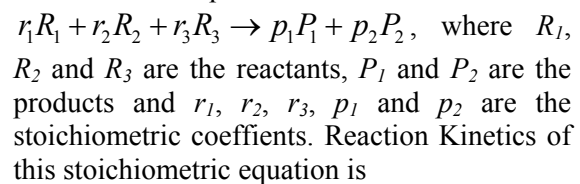
$$\frac{d[B]}{dt} = k \cdot [B] \cdot [N_l], \quad \text{where } k \text{ is a rate}$$

coefficient that depends on physiochemical variables such as temperature, dissolved oxygen and stirrer speed.

### 2.3. Reaction Kinetics

Reaction Kinetics is used to model the synthesis of xanthan.

The following equation is an example of a stoichiometric equation:



$$\begin{aligned} v &= -\frac{1}{r_1} \frac{d[R_1]}{dt} = -\frac{1}{r_2} \frac{d[R_2]}{dt} = -\frac{1}{r_3} \frac{d[R_3]}{dt} \\ &= \frac{1}{p_1} \frac{d[P_1]}{dt} = \frac{1}{p_2} \frac{d[P_2]}{dt} \\ &= k \cdot [R_1]^{s_1} \cdot [R_2]^{s_2} \cdot [R_3]^{s_3}, \end{aligned}$$

where  $k$  is a rate constant.

### 2.4. Petri Nets

A Petri Net is a graphical construction to describe and analyze concurrent processes and non-deterministic procedures. It is a graph with two different kinds of nodes: Places and Transitions, whereas only a Place can be connected with a Transition or a Transition with a Place. Every Place contains an integer number of Tokens and every edge has a

weighting. A Transition is ready to fire when every Place in its previous area has at least as many Tokens as the appropriate edge weighting shows. A Transition that is ready to fire fires by removing as many Tokens as the respective edge weighting indicates - from all of the Places in its previous area. In addition, a specific number of Tokens is stored in all of the Places of its past area - according to the specific edge weighting. To model biological systems, the Petri Net concept has been extended to stochastic Petri Nets, continuous Petri Nets and hybrid Petri Nets, cf [6].

### 2.5. Petri Net Library

Petri Nets are ideal to model biological processes. Thereby, metabolites, enzymes and genes are modeled with Places, and Transitions represent the reactions between them [7]. In the following it is described how the existing Petri Net Libraries were extended [6]:

- Continuous Petri Net elements were implemented because biochemical reactions, which convert one substance to another, proceed continuously.
- The speed of these reactions depends mostly on the current concentration of specific substances [8], which can be now displayed by dynamic edge weightings.
- It should be possible to model gene regulation, which contains discrete processes as well as continuous ones. Hybrid Petri Nets, which comprise both discrete and continuous Petri Net elements [9], are now able to fulfil this task.
- The edges can also have upper and lower boundaries. This is necessary for modeling substances which only react when a specific concentration is reached.

The Petri Net Library is structured in seven sub-libraries: Discrete, Continuous, Stochastic, Reactions, Interfaces, Constants, and Functions (see Figure 3).

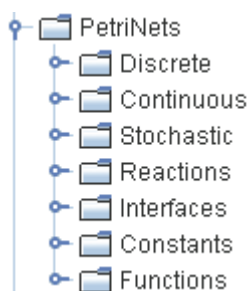


Figure 3: Structure of the Petri Net Library

The next figure shows the icons for discrete, continuous and stochastic Petri Nets elements. For additional information about the functionality, application and implementation of these Petri Net elements see [6]. This paper focuses on the Reaction Library.

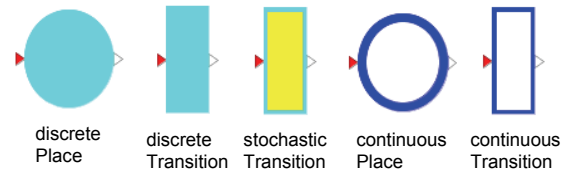


Figure 4: Icons of the Petri Net elements

### 2.6. Reaction Library

Petri Net elements have been wrapped into appropriate models for different kinds of reactions to simplify the modeling process. These reactions are organized in a sub-library of the Petri Net Library called 'Reactions' (see Figure 3). This library is again divided in different sub-libraries to classify the reactions (see Figure 5). These are:

- Reaction Kinetics
- Enzyme Kinetics
- Growth Kinetics.

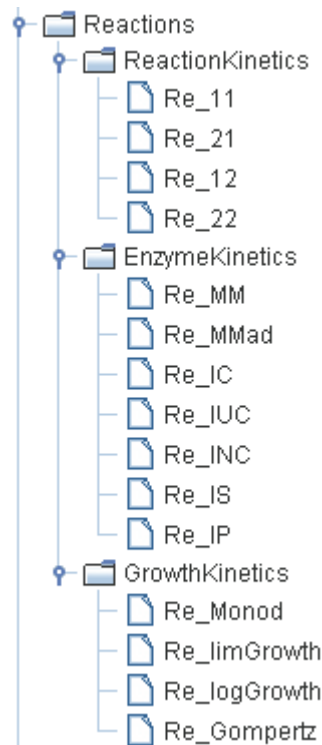


Figure 5: Structure of the Reactions Library

### 2.6.1. ReactionKinetics Library

The ReactionKinetics sub-library comprises reactions with the Reaction Kinetics as edge weightings for one or two reactants and one or two products. The reactions for more reactants or products can be extended easily. The reaction  $r_1R_1 + r_2R_2 \rightarrow p_1P_1$  for example can be modeled by the reaction Re\_21 (see Figure 6).



Figure 6: The icon of the reaction Re\_21 of the ReactionKinetics Library

The next figure shows the property-dialog of reaction Re\_21. The rate constant  $k$  and the stoichiometric coefficients  $r_1$ ,  $r_2$  and  $p_1$  can be keyed in.

|                                               |                                                    |             |
|-----------------------------------------------|----------------------------------------------------|-------------|
| k: "rate constant"                            | <input type="text" value="1"/>                     | Default: 1  |
| r1: "stoichiometry coefficient of reactant 1" | <input type="text" value="1"/>                     | Default: 1  |
| r2: "stoichiometry coefficient of reactant 2" | <input type="text" value="1"/>                     | Default: 1  |
| p1: "stoichiometry coefficient of product 1"  | <input type="text" value="1"/>                     | Default: 1  |
| comment: ""                                   | <input style="width: 100%;" type="text" value=""/> | Default: "" |

Figure 7: Property-dialog of the reaction Re\_21

### 2.6.2. EnzymeKinetics Library

The EnzymeKinetics Library consists of reactions that are performed with the aid of enzymes:

- Michaelis-Menten Kinetics (Re\_MM)
- Reversible Michaelis-Menten Kinetics (Re\_MMad)
- Competitive enzyme inhibition (Re\_IC)
- Uncompetitive enzyme inhibition (Re\_IUC)
- Non-competitive enzyme inhibition (Re\_INC)
- Substrate inhibition (Re\_IS)
- Product inhibition (Re\_IP)

For more information about the kinetics and enzyme inhibition see [10].

Figure 8 shows a metabolism reaction modeled with the Michaelis-Menten-Kinetics. The icons *sub* and *pro* are Places of the sub-library 'Continuous' of the Petri Net Library, and the Michaelis-Menten reaction between them can be found in the EnzymeKinetics Library.

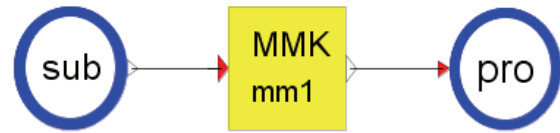


Figure 8: A reaction modeled with the Michaelis-Menten Kinetics

The turnover number  $k_{cat}$ , the Michaelis-Menten constant  $K_m$  and the enzyme concentration can be entered in the property-dialog (see Figure 9).

|                                 |                                                    |              |
|---------------------------------|----------------------------------------------------|--------------|
| kcat: "turn over number"        | <input type="text" value="1"/>                     | Default: 1   |
| Km: "Michaelis-Menten constant" | <input type="text" value="1"/>                     | Default: 1   |
| e_con: "enzyme concentration"   | <input type="text" value="0.1"/>                   | Default: 0.1 |
| ec_number: "ec-number"          | <input style="width: 100%;" type="text" value=""/> | Default: ""  |

Figure 9: Property-dialog of the Michaelis-Menten Kinetics

The following figure displays the wrapping process of the reaction in Figure 8. The model 'Re\_MM' consists of a continuous Transition of the Continuous Library with the Michaelis-Menten Kinetics as edge weightings. The edge weightings in continuous Petri Nets are the right sides of a differential equation.

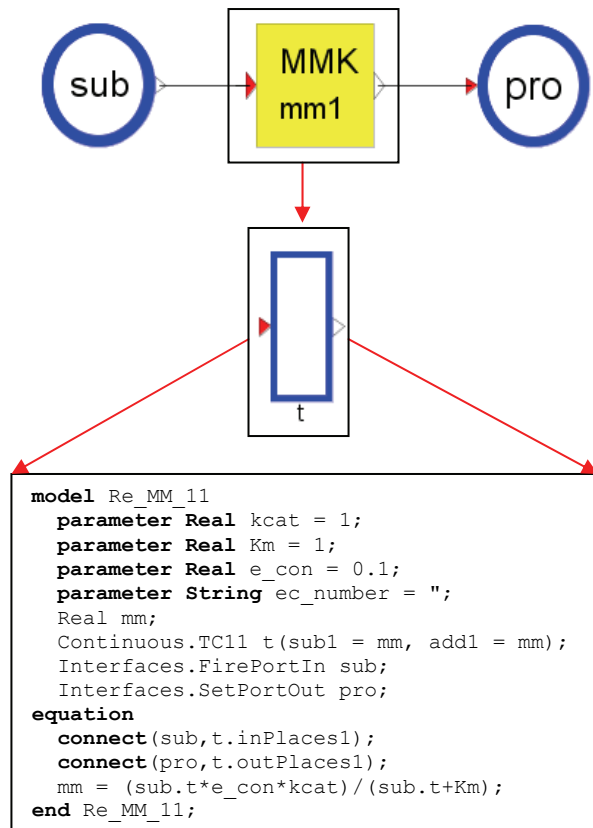


Figure 10: Wrapping of the Michaelis-Menten-Kinetics

### 2.6.3. GrowthKinetics Library

Reactions for modeling growth are organized in the ReactionKinetics Library with two reactions for limited growth:

- Monod Kinetics (Re\_Monod)
  - Limited Growth Kinetics (Re\_limGrowth)
- and two for unlimited growth:
- Logistic Growth Kinetics (Re\_logGrowth)
  - Gompertz Kinetics (Re\_Gompertz) [11].

In the case of limited growth the decrease of the limited nutrient is modeled with the differential equation

$$\frac{d[N_i]}{dt} = -\frac{1}{Y_{BN_i}} \cdot \frac{d[B]}{dt},$$

where  $[N_i]$  is the

concentration of the limited nutrient,  $[B]$  is the biomass concentration and  $Y_{BN_i}$  is the macroscopic yield of biomass per nutrient unit.

Figure 11 shows an example for modeling with the Monod Kinetics, the nutrient and the biomass are Places of the Continuous Library.



Figure 11: An example for modeling with the Monod Kinetics

The parameters for the Monod Kinetics can be entered in the property-dialog (see Figure 12).

|                                    |   |            |
|------------------------------------|---|------------|
| m : "maximum specific growth rate" | 1 | Default: 1 |
| Kn : "Monod constant"              | 1 | Default: 1 |
| Ybn : "yield coefficient"          | 1 | Default: 1 |

Figure 12: Property-dialog of the Monod Kinetics (Re\_Monod)

## 2.7. Database Integration

Rafael Friesen has developed a database connection to BRENDA in his master thesis [12], which allows an easy and fast model integration of kinetic data. For using this database connection in combination with the Petri Net Library, a special SimForge version is necessary. Figure 13 shows the new property-dialog of the Michaelis-Menten reaction (Re\_MM). Next to the parameters *kcat* and *km* two additional fields show the EC-number filled in at the bottom.

|                                  |           |                                      |              |
|----------------------------------|-----------|--------------------------------------|--------------|
| kcat : "turn over number"        | 1         | 1.1.1.1                              | Default: 1   |
| Km : "Michaelis-Menten constant" | 1         | 1.1.1.1                              | Default: 1   |
| e_con : "enzyme concentration"   | 0.1       |                                      | Default: 0.1 |
| ec_number : "ec-number"          | *1.1.1.1* | <a href="#">BRENDA Internet Link</a> | Default: **  |

Figure 13: Property-Dialog of the Michaelis-Menten reaction (Re\_MM)

If you press 'enter' in these fields next to the *kcat* or *km* values, the following selection dialog appears.

Figure 14: Selection dialog

Firstly, the modeled organism can be chosen. In the selection list all organisms with at least one *kcat* or *km* value in the database BRENDA appear.

Figure 15: Organism selection

After the organism selection it is possible to choose a proper value. Next to the respective value information about the substrate and experimental conditions is given.

Figure 16: Value selection

If you press 'Apply' the value will appear in the property-dialog of the Michaelis-Menten reaction.

Similarly, you can integrate the dissociation constants of the inhibition reactions.

## 3. Modeling Xanthan Production

With the aid of the model of the present paper, it is possible to predict biomass and xanthan concentrations of the bacterium *Xanthomonas campestris* pv. *campestris* (Xcc), by a given

initial glucose concentration. Both, the growth and the xanthan production, are limited by glucose. Figure 17 shows the model on the top level and Figure 18 shows the Xcc-model, the model behind the grey icon with the denotation 'Xcc'.

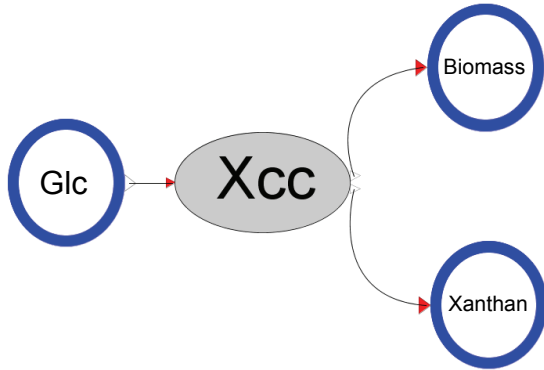


Figure 17: Model on the top level

As can be seen in Figure 18, the bacterium has two choices after glucose intake: It can either opt for growth or for xanthan production.

Xanthan consists of five components: UDP-glucose, UDP-glucuronic acid, GDP-mannose, pyruvate and acetate, the model, however, confines to the three nucleotide sugars (UDP-glucose, UDP-glucuronic acid, GDP-

mannose). The synthesis of these three nucleotide sugars to xanthan is modeled with Reaction Kinetics (cf. section 2.3), with one xanthan unit consisting of two units UDP-glucose, one unit UDP-glucuronic acid and two units GDP-mannose.

The growth is modeled with the limited Growth Kinetics and Monod Kinetics for reasons of comparison (cf. section 2.2). The conversion process glucose to biomass is split up into two sub-processes.

The edge weightings of the transition *glcOutIn* are:

$$\text{add1} = \text{sub1} = \text{kg} * \text{der}(\text{Biomass.t})$$

and of transition *growth*:

$$\text{add1} = \text{sub1} = \text{kb} * \text{glcIn.t}$$

(limited Growth Kinetics)

$$\text{add1} = \text{sub1} = \text{mb} * \text{glcIn.t} / (\text{Kmb} + \text{glcIn.t})$$

(Monod Kinetics).

The conversion from one metabolite to another is modeled by the Michaels-Menten Kinetics (cf section 2.1) from the EnzymeKinetics Library and all metabolites are modeled by continuous Places from the Continuous Library.

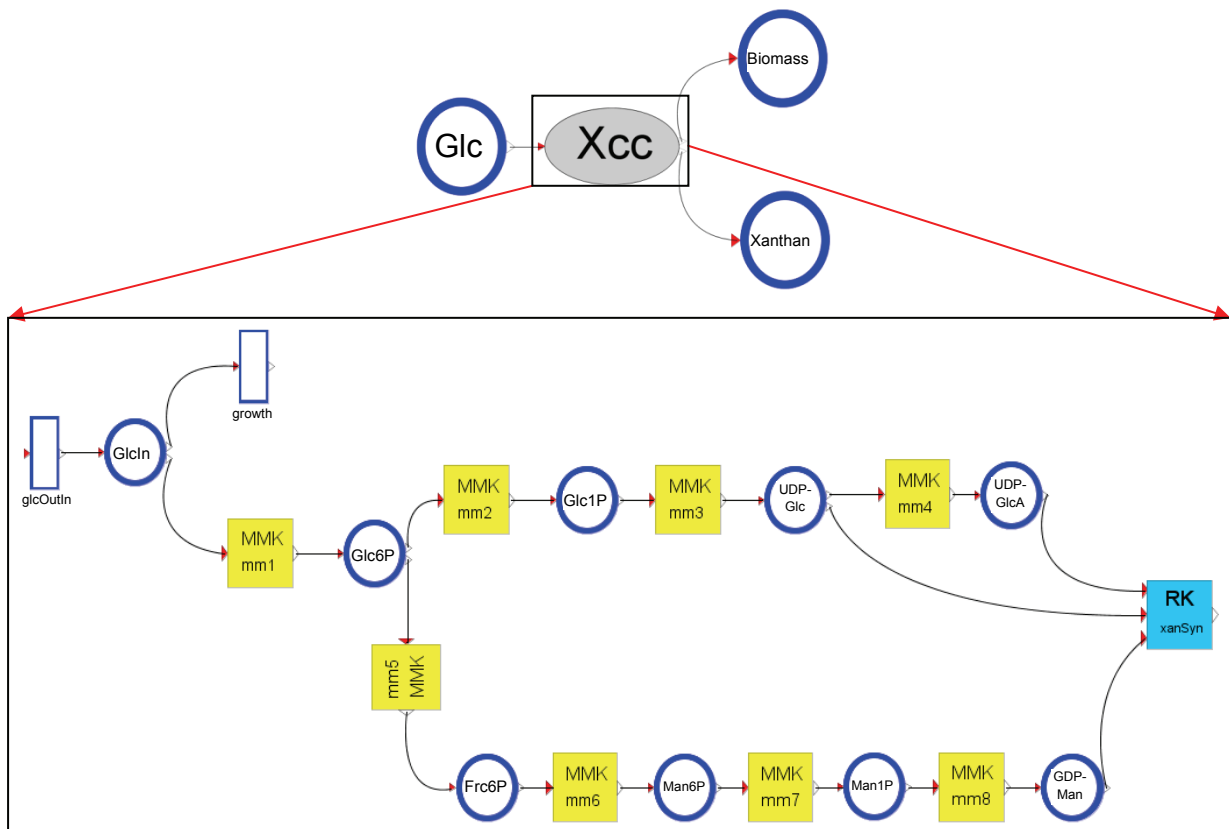


Figure 18: Sub-Model Xcc

## 4. Experimental Data

To adapt the model parameters to the reality a fermentation was made by Tony Watt [13] under industrial conditions. The bacteria grew in a fermenter with an initial glucose concentration of 12.57 g/l.

For the validation of the model an additional fermentation was made by Tony Watt in a fermenter with an initial glucose concentration of 13.75 g/l.

In both fermentation experiments the xanthan-, biomass-, and glucose-concentrations were measured at several time points.

## 5. Data-Fitting

The model parameters were fitted to the data of the first fermentation using the MATLAB optimization toolbox. At first, the model of Figure 18 was simplified into a smaller sub-model to estimate the first set of parameters (see Figure 19). These are  $kb$  for the limited Growth Kinetics,  $mb$  and  $Kmb$  for the Monod Kinetics,  $kg$  for the edge weighting of the transition  $glcOutIn$ , and the two parameters  $kcat1$  and  $km1$  of the Michaelis-Menten reaction  $mm1$ , respectively. The measured concentrations were glucose and biomass. The concentrations of the glucose inside the bacteria (GlcIn) and of glucose-6-phosphate (Glc6P) were unknown.

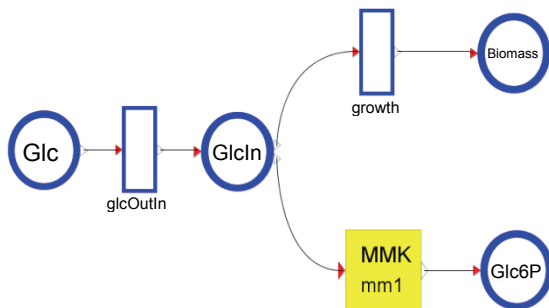


Figure 19: First sub-model for the parameter estimation

The following figures show the results of the adapted biomass concentrations, with Figure 20 displaying the results of the model with the limited Growth Kinetics and Figure 21 representing the model with the Monod Kinetics. Both show a good agreement with the experimental data.

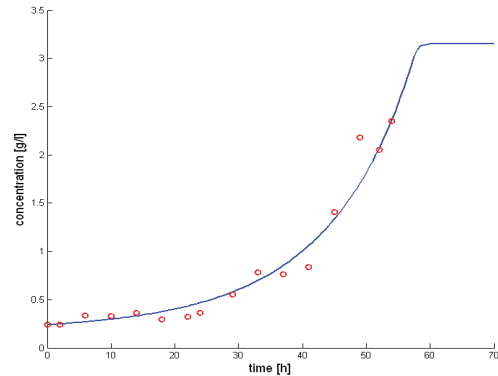


Figure 20: Data-fitting of biomass (limited Growth Kinetics)

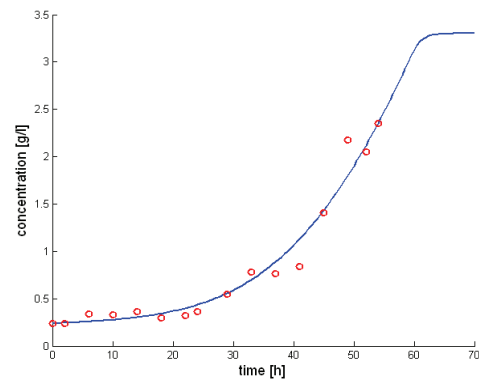


Figure 21: Data-fitting of biomass (Monod Kinetics)

For the next optimization steps the limited Growth kinetics was chosen. Figure 22 shows the data-fitted glucose concentration of this model.

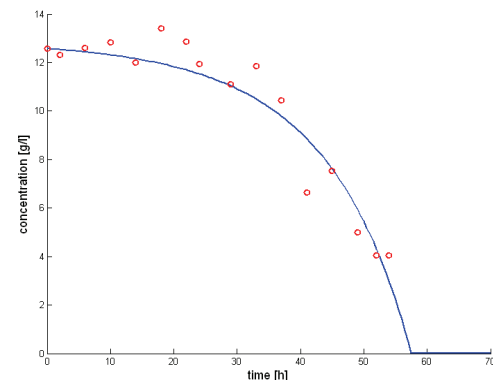


Figure 22: Data-fitting of glucose

The four parameters ( $kb$ ,  $kg$ ,  $kcat1$  and  $km1$ ) are now fixed and the sub-model of Figure 19 is expanded to estimate the concentrations for the three nucleotide sugars that are necessary to produce the experimental xanthan concentration results (see Figure 23). In this optimization step intermediate metabolites have been left out.

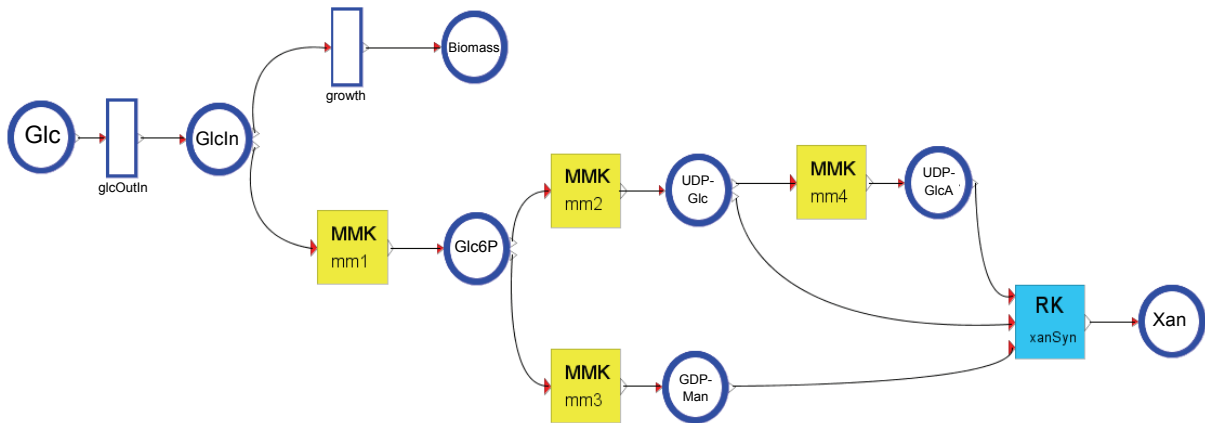


Figure 23: Second sub-model for the parameter estimation

Additionally, the kinetic parameters for the conversion from UDP-glucose (UDP-Glc) to UDP-glucuronic acid (UDP-GlcA) are determined.

Figure 24 displays the results of the data-fitting for the xanthan concentration. Now the  $k_{cat}$  and  $k_m$  values for the conversion from UDP-glucose to UDP-glucuronic acid are fixed and the concentrations of the three nucleotide sugars are saved.

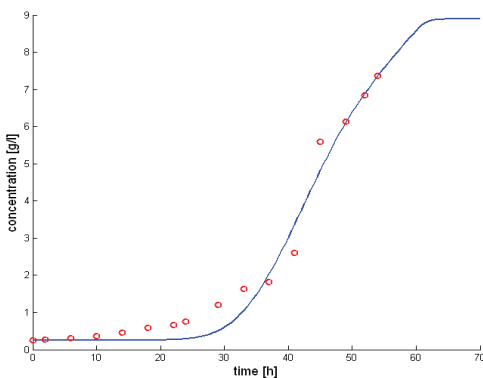


Figure 24: Data-fitting of xanthan

The  $k_{cat}$  and  $k_m$  values for the intermediate metabolites are finally estimated in the last optimization step. These are twelve additional parameters which are adapted to the nucleotide sugar concentrations of the previous optimization step. Figure 25 shows the predicted concentrations of the metabolites for the metabolism in Figure 18.

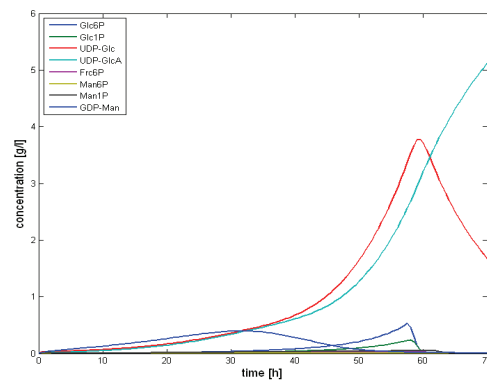


Figure 25: Concentrations of the metabolites

With a data-fitted model at hand, it is now possible to predict biomass growth and xanthan production with different initial glucose concentrations. Figure 26 shows the biomass concentrations for the initial glucose concentrations 3 g/l, 6 g/l, 8 g/l and 10 g/l. Figure 27 presents the corresponding xanthan concentrations.

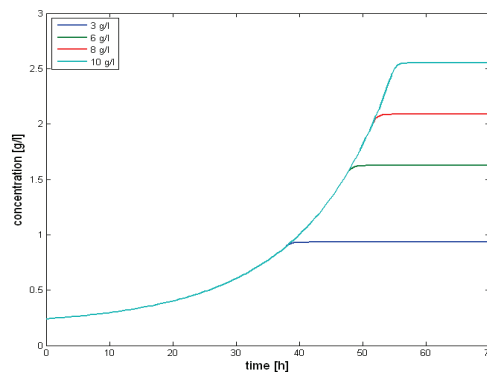


Figure 26: Influence of initial glucose concentration on evolution of **biomass** concentration



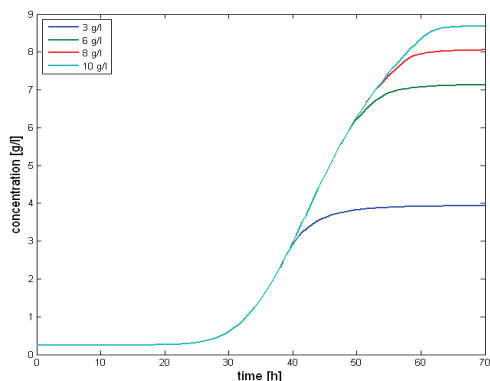


Figure 27: Influence of initial glucose concentration on evolution of **xanthan** concentration

For the validation of the model an additional fermentation was made. The predicted model curves of glucose, biomass and xanthan show a good agreement with the experimental data (see Figure 28, Figure 29, Figure 30).

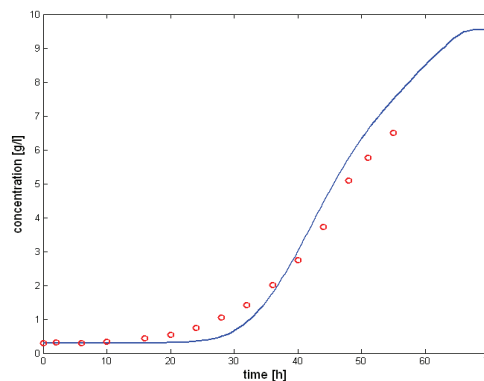


Figure 30: Experimental and model-predicted **xanthan** concentration of the second fermentation

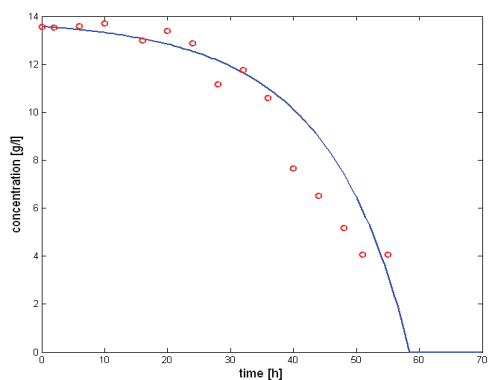


Figure 28: Experimental and model-predicted **glucose** concentration of the second fermentation

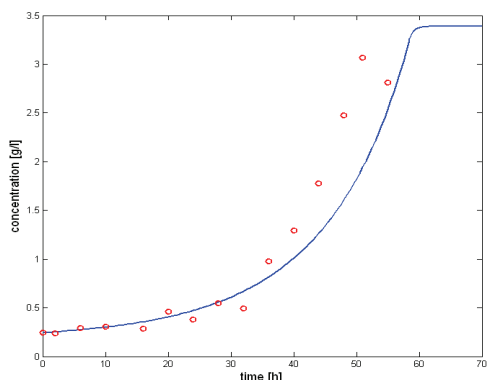


Figure 29: Experimental and model-predicted **biomass** concentration of the second fermentation

## 6. Conclusion and Outlook

For modeling biological systems, a Petri Net Library was implemented in OpenModelica with the SimForge GUI. To simplify the modeling process, the Petri Net elements were wrapped into reaction models for different application areas: Reaction Kinetics, Enzyme Kinetics and Growth Kinetics.

With the aid of this library a model was developed for predicting biomass and xanthan concentrations for the bacterium *Xanthomonas campestris* pv. *campestris* given an initial glucose concentration.

The respective model parameters were estimated stepwise by using the MATLAB Optimization toolbox. Validation tests demonstrate a good agreement with measured fermentation data. In the future more experiments are planned to achieve an even better adaptation. Additionally, not only xanthan, biomass and glucose will be measured but also the concentrations of the corresponding metabolites. This measurement is possible with a gas-phase chromatograph that is coupled to a mass spectrometer, the so-called GC/MS analysis. This method allows to determine the concentrations of the metabolites Glucose-6-Phosphate, Glucose-1-Phosphate, Fructose-6-Phosphate, Mannose-6-Phosphate, and Mannose-1-Phosphate.

Furthermore, the quantification of the nucleotide sugars of xanthan can be achieved using high performance liquid chromatography (HPLC). Last but not least further extensions of the model will be considered, i.e. modeling nitrogen as growth limiting factor.

## References

- [1] **Garcia-Ochoa, F., et al.** Xanthan gum: production, recovery, and properties. *Biotechnology Advances*. 2000, 18, pp. 549-579.
- [2] **Vorhölter, Frank-Jörg, et al.** The genome of *Xanthomonas campestris* pv. *campestris* B100 and its use for the reconstruction of metabolic pathways involved in xanthan biosynthesis. *Journal of Biotechnology*. 2008, pp. 33-45.
- [3] **Garcia-Ochoa, F., Santos, V. E. and Alcon, A.** Structured kinetic model for *Xanthomonas campestris* growth. *Enzyme and Microbial Technology*. 2004, pp. 583-594.
- [4] **Monod, Jacques.** The Growth of Bacterial Cultures. *Annual Review of Microbiology*. 1949, pp. 371-394.
- [5] **Quinlan, Alicia V.** Kinetics of Secondary Metabolite Synthesis in Batch Cultures When Two Different Substrates Limit Cell Growth and Metabolite Production: Xanthan Synthesis by *Xanthomonas campestris*. *Biochemical Eng.* 469, 1986, pp. 259-269.
- [6] **Proß, Sabrina and Bachmann, Bernhard.** A Petri Net Library for Modeling Hybrid Systems in OpenModelica. *submitted (Modelica Conference 2009)*. 2009.
- [7] **Reddy, Venkatramana N., Liebman, Michael N. and Mavrovouniotis, Michael L.** Qualitative Analysis of Biochemical Reaction Systems. *Compu. Biol. Med.* 1996, pp. 9-24.
- [8] **Hofestädt, R. and Thelen, S.** Quantitative Modeling of Biochemical Networks. *In Silico Biology*. 1998, 1, pp. 39-53.
- [9] **Doi, Atsushi, et al.** Constructing biological pathway models with hybrid functional Petri nets. *In Silico Biology*. 2004.
- [10] **Berg, Jeremy M., Tymoczko, John L. and Stryer, Lubert.** *Biochemistry*. New York : W. H: Freeman, 2006.
- [11] **Gompertz, Benjamin.** On the nature of the function expressive of the law of human mortality, and on a new mode of determining the value of life contingencies. *Phil. Trans. R. Soc. Lond.* 115, pp. 513-585.
- [12] **Friesen, Rafael.** Petrinets in systems biology: Modelling cell communication with petri nets. Bielefeld, 2009.
- [13] **Watt, Tony.** private communication. Bielefeld, 2009.